POLARIZATION OF THE COSMIC BACKGROUND RADIATION

PHILIP M. LUBIN AND GEORGE F. SMOOT
Space Sciences Laboratory and Lawrence Berkeley Laboratory, University of California at Berkeley
Received 1980 August 18; accepted 1980 October 14

ABSTRACT

We discuss the technique and results of a measurement of the linear polarization of the cosmic background radiation at a wavelength of 9 mm. Data taken between 1978 May and 1980 February from both the northern hemisphere (Berkeley latitude 38° N) and the southern hemisphere (Lima latitude 12° S) over 11 declinations from $-37°$ to $+63°$ show the radiation to be essentially unpolarized over all areas surveyed. Fitting all data gives the 95% confidence level limit on a linearly polarized component of 0.3 mK for spherical harmonics through third order. A fit of all data to the anisotropic axisymmetric model of Rees yields a 95% confidence level limit of 0.15 mK for the magnitude of the polarized component. Constraints on various cosmological models are discussed in light of these limits.

Subject headings: cosmic background radiation — cosmology – polarization

I. INTRODUCTION

The cosmic background radiation, discovered by Penzias and Wilson (1965), has profoundly influenced our understanding of the universe: it is thought to be the relic radiation of the primordial fireball, emitted within minutes of the big bang. The study of this radiation is a unique probe into the structure of the universe.

The cosmic background radiation field can be characterized at a fixed point in space in terms of its (1) spectrum $E(\kappa, \bar{\omega})$, (2) angular distribution $E(\bar{\kappa}, \omega)$, and (3) polarization state $\bar{E}(\kappa, \omega)$, where κ is the wave vector and ω is the angular frequency.

Our current understanding of the spectrum is that it is essentially a blackbody with a characteristic temperature about 3 K with a possible deviation ($\sim 15\%$) near the peak (Woody and Richards 1979). The angular distribution of the radiation is nearly isotropic with a deviation of amplitude ~ 3 mK (0.1%) interpreted as being due to the motion of the Earth through the radiation field (Corey and Wilkinson 1976; Smoot, Gorenstein, and Muller 1977). After removal of this "first order anisotropy" no residual anisotropy is seen with a 95% confidence level of 1 mK for quadruple terms (Cheng *et al.* 1979; Smoot and Lubin 1979; Gorenstein and Smoot 1981) except for a recent report by Fabbri *et al.* (1980) and Boughn,

Cheng, and Wilkinson (1981) of a possible quadrupole component at the level of 1 mk.

Although Rees (1968) suggested that anisotropic expansion of the universe could yield a net linear polarization in the cosmic background radiation, little attention has been directed toward using polarization measurements to search for anisotropies. In 1972, George Nanos (1974, 1979), under Dave Wilkinson at Princeton, initiated an experiment to search for linear polarization with a null result. In addition, Caderni *et al.* (1978a) reported no net linear polarization from a balloon-borne infrared experiment. Unfortunately the balloon flight was terminated prematurely, and only a small portion of the sky was surveyed. Table 1 summarizes the previous measurements.

a) Anisotropies

There are two basic classes of anisotropies: those intrinsic to the radiation and those extrinsic in origin. The extrinsic anisotropies are typified by the first order anisotropy caused by the motion of the observer through the radiation.

If an intrinsic intensity anisotropy exists in the cosmic background radiation, then the radiation can acquire a net linear polarization by Thomson scattering from

TABLE 1

MEASURED LIMITS ON LINEAR POLARIZATION (95% confidence level)

Reference	Wavelength (cm)	Sky Coverage	Limit
Penzias and Wilson 1965	7.35	scattered	10%
Nanos 1974, 1979	3.2	declination = $+40°$	0.06%
Caderni *et al.* 1978	0.05–0.3	near galactic center	0.1–1%
Lubin and Smoot 1979	0.91	declinations 38°, 53°, 63°	0.03%
This work	0.91	11 declinations $-37°$ to $+63°$	0.006%

1

electrons in ionized matter. *Any intrinsic anisotropy is therefore accompanied by a net polarization, if the anisotropy originated before the last scattering.* Extrinsic types of anisotropies are generally not accompanied by a net polarization. Table 2 gives those types of anisotropies expected to produce polarization.

In general, intrinsic anisotropies are expected to exist, although their level is uncertain. From causality arguments, anisotropies should arise because widely separated parts of the universe have always been out of communication with other parts. In simple models, anisotropy is expected on an angular scale size characterized by $\theta_c = 4°2(q_0)^{1/2}$, where q_0 is the deceleration parameter (Weinberg 1972). If $q_0 = 0.5$ (minimum needed for closed universe), then $\theta_c = 3°$. Anisotropic expansion of the universe causes an anisotropy because the universe expands more rapidly in some directions than in others, and thus radiation is redshifted by differing amounts in different directions. Figure 1 shows the polarization pattern expected for two cases of an axisymmetric expansion. If the universe were rotating, then an intrinsic anisotropy would also be expected (Hawking 1969). Anisotropy measurements and therefore polarization measurements provide a test of Mach's principle (Mach 1893).

Studying the polarization properties of the radiation serves a dual purpose: it measures possible inherent polarization that may exist while being insensitive to local causes of anisotropy such as our motion, and it provides a secondary means of searching for any intrinsic anisotropy in intensity. In addition, the discovery of both intensity and polarization anisotropies and a measurement of their relative magnitudes provides information about the intergalactic medium and its ionization history.

Polarization measurements also provide a check of the first order anisotropy seen in intensity. If the anisotropy is due to our motion, no net polarization is expected; however, if this first order anisotropy is intrinsic to the radiation itself, in part or in total, a net polarization could exist. So a null result tends to support the interpretation of the intensity anisotropy as being locally induced by our motion.
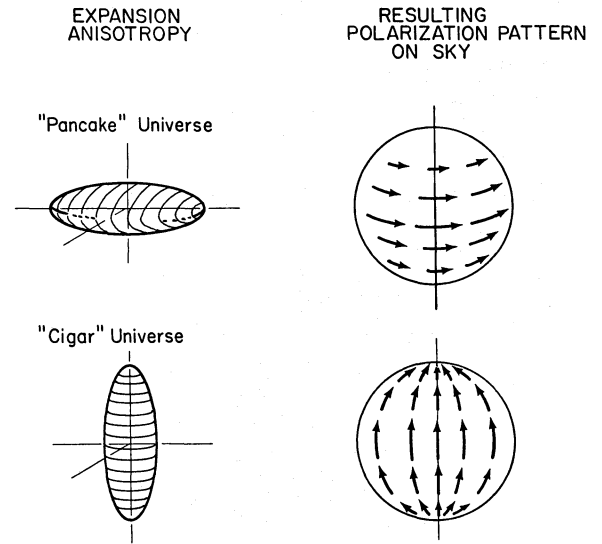
TABLE 2

POSSIBLE CAUSES OF ANISOTROPY AND POLARIZATION IN THE
3 K COSMIC BACKGROUND RADIATION

Cause of Anisotropy	Type	Polarization?
Motion of observer	Local	No
Rotation of universe	Intrinsic	Yes
Long wavelength gravity waves	Intrinsic	Yes
Anisotropic expansion (shear)	Intrinsic	Yes
Density inhomogeneities:		
a) Primordial	Intrinsic	Yes
b) Local	Local	No
Motion of source	Intrinsic	Yes
Transverse motion of clusters	Local	Yes

FIG. 1.—Expansion anisotropy and resulting polarization pattern on the sky for two simple axisymmetric anisotropic models.

II. ANTENNA TEMPERATURE AND STOKES PARAMETERS

The experiment has been designed to measure the Stokes parameters of linear polarization Q and U for the cosmic background radiation.

For blackbody radiation of temperature T, and flux I is given by:

$$I = \frac{2h\nu^3}{c^2} \frac{1}{e^{h\nu/kT} - 1} \text{ ergs cm}^{-2} \text{ s}^{-1} \text{ sr}^{-1} \text{ Hz}^{-1} \quad (1)$$

For $h\nu \ll kT$ (the Rayleigh-Jeans limit) this reduces to:

$$I = 2kT/\lambda^2 . \quad (2)$$

For a given flux I (ergs cm^{-2} s^{-1} sr^{-1} Hz^{-1}), the antenna temperature T_A is defined such that, in the Rayleigh-Jeans limit, the flux produced by a blackbody of temperature T_A would produce the given flux I. Because microwave radiometers measure flux, it is convenient to define an equivalent temperature T_A as:

$$T_A = \frac{\lambda^2}{2k} I . \quad (3)$$

Using (1) for I gives:

$$T_A = \frac{x}{e^x - 1} T, \qquad x = \frac{h\nu}{kT} . \quad (4)$$

Also,

$$\frac{dT_A}{dT} = \frac{x^2 e^x}{(e^x - 1)^2} . \quad (5)$$

The antenna temperature at $\nu = 33$ GHz for $T = 2.7$ K is:

$$T_A = 2.0 \text{ K} \quad \text{while} \quad \frac{dT_A}{dT} = 0.98 . \quad (6)$$

In terms of antenna temperature Q and U are defined as follows:

$$Q = T_{NS} - T_{EW} , \qquad (7)$$

$$U = T_{NW,SE} - T_{NE,SW} , \qquad (8)$$

where T_{NS} = antenna temperature of radiation polarized along the north-south direction; T_{EW} = antenna temperature of radiation polarized along the east-west direction; $T_{NW,SE}$ = antenna temperature of radiation polarized along the northwest-southeast direction; and $T_{NE,SW}$ = antenna temperature of radiation polarized along the northeast-southwest direction.

Stokes parameters are ideally suited for this experiment since the measured quantities differ from the Stokes parameters by a simple scale factor.

If the measuring instrument is initially aligned to measure Q, rotation of the instrument by 45° gives U, while a rotation by 90° reverses the sign of the measured parameter. Most instrumental effects are either constant with rotation or change sign under rotation by 180°. Rotating in 45° increments through a full 360° will therefore measure Q and U as well as the instrumental effects. This is a crucial aspect of the experiment, since we are attempting to measure polarization to a level which is one one-hundredth of the instrumental effect and one ten-thousandth of the intensity of the cosmic background radiation.

III. EXPERIMENTAL APPARATUS AND PROCEDURES

The apparatus is shown schematically in Figure 2. The 9.1 mm Dicke radiometer uses a Faraday rotation switch to switch between polarization states. The antenna axis can tilt relative to vertical in order to observe various declinations from a fixed latitude. The ground shield aids in rejecting radiation from nearby objects. A stepping motor rotates the radiometer about its axis to allow both Stokes parameters Q and U to be measured and to provide a basic symmetry in order to cancel instrumental effects. A rain shield of 0.5 mil polyvinylidene (Saran Wrap) provides protection from rain and dust.

a) Microwave Radiometer

The radiometer includes a superheterodyne microwave receiver operating at 9.1 mm wavelength which is rapidly switched between two orthogonal polarization states, giving an output voltage proportional to the power difference in these two polarization states. As with all receivers, the instrument has a sensitivity limited by its intrinsic noise. The rms output temperature fluctuations ΔT, measured by a square-wave switched, narrow-band detected radiometer, are $\Delta T = 2.2 T_{sys}/(B\tau)^{1/2}$ where T_{sys} is the system noise temperature (characteristic of system performance), B is the IF bandwidth, and τ is the measurement time (Kraus 1966). For our instrument, the system noise temperature is typically $T_{sys} = 520$ K and the IF bandwidth is $B = 500$ MHz, so $\Delta T = 52$ mK s$^{-1/2}$. Thus, by measuring for a sufficient period of time the desired sensitivity can be obtained. For example, a 1 year integration provides a theoretical sensitivity of 0.01 mK.
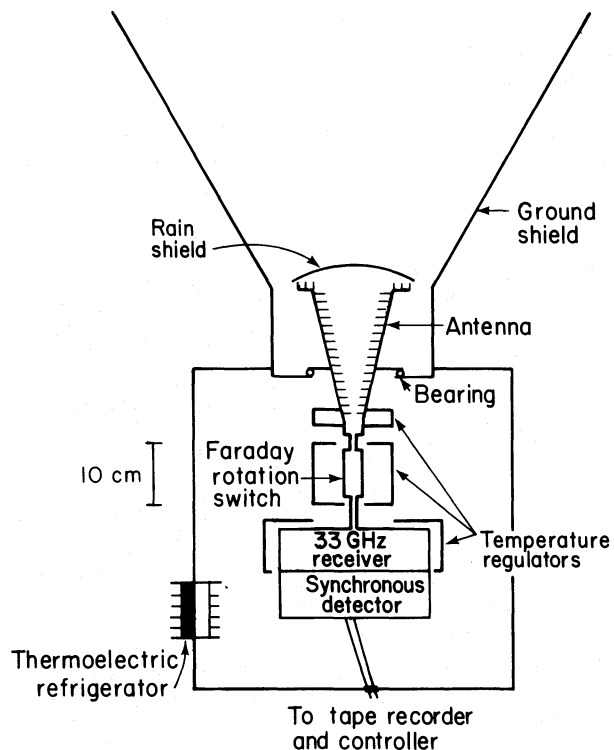

Fig. 2.—Schematic of microwave polarimeter used.

The radiometer is encased in a metal can which provides RF shielding. The radiometer is electrically insulated from the can, decoupling any possible grounding effects. The lock-in amplifier uses an "ideal" integrator and a narrow-band amplifier ($Q = 10$) with a center frequency of 100 Hz, and it responds only to signals synchronous with the switching of the Faraday rotation switch. The output of the lock-in is digitized and recorded on a remote tape recorder. Because the distance from radiometer to tape is typically 100 feet or more, a shielded twisted-pair line driver-receiver system is used to transmit and receive the data. This has the added virtue of eliminating any ground loops between the tape recorder and radiometer.

b) Thermal Regulation

Thermal regulation of the instrument is crucial because the various components, particularly the Faraday rotation switch, are sensitive to temperature variations. As shown in Figure 2, we thermally regulate three sections: the lower portion (throat) of the antenna, the Faraday rotation switch, and the microwave receiver. In addition, the lock-in amplifier is temperature stabilized through attachment to the regulated block of the receiver.

Regulation is achieved by a combination of active and passive thermal elements. The three regulated areas have independent linear proportional heaters with feedback from sensors at the critical points, achieving a typical thermal regulation of $\pm 0.2°$ C. Large thermal capacity in the form of aluminum blocks assures that heat is evenly

distributed with a long time constant so that the time rate of change of the temperature is less than 0.3° C per hour. An analysis of the temperature stability of the components, shows that the temperature changes cause less than 0.06 mK error in Q and U (Lubin 1980a). A thermoelectric refrigerator ensures that regulation is achieved even during periods of warm weather.

c) Calibration

Calibration is periodically performed using a polarized blackbody source at ambient temperature. The calibrator is shown in Figure 3. Theoretical calculations (Chu, Gans, and Legg 1975) and our own radiometric measurements show that the calibrator is nearly ideal in that the polarized signal is equal to the difference in temperature between the reference blackbody (Eccosorb) and the sky. The system is sufficiently stable that over several weeks the calibration changes by less than 2%.

The wire grid in the calibrator is made of photo-etched copper-plated 2 mil Kapton. The wires are spaced 0.64 mm on center. This dimension is not critical as long as it is small compared to the wavelength of 9.1 mm. The grid is canted at a 45° angle. Radiation whose electric field (polarization) is along the wire direction will be reflected, whereas radiation polarized perpendicularly will be transmitted. This is precisely analogous to the optical case of a Polaroid sheet, where the conductive wires are provided by iodine ions on a stretched polymer grid (Shurcliff and Ballard 1962).

The calibration signal seen by the polarimeter is a partially polarized signal, the magnitude of the polarized part being the difference in temperature between the Eccosorb (ambient temperature blackbody source) and the sky (atmosphere plus background radiation). Independent measurements of the atmospheric contribution give $T_A \sim 12 \pm 1$ K for a typical clear day. The presence of variable amounts of water vapor can change this by several kelvins. Adding the 2 K contribution of the cosmic background radiation yields a sky temperature of $T_A = 14(+4, -1)$ K, where the skewed error is due to the variability of water vapor in the atmosphere.

Independent radiometric measurements at 33 GHz give an insertion loss through the grid of $1.5 \pm 0.1\%$ for the transmission mode and reflection of $99 \pm 1\%$ in the reflection mode. The Eccosorb temperature is measured for each calibration with an error of less than 1%. The total polarized signal is then $T_{cal} = T_{Ecc} - 14$ K with an error of less than 4%. An additional calibration using the same receiver, but replacing the Faraday rotation switch with a Dicke switch, is in agreement to within 5%.

d) Data Acquisition

The radiometer signal is integrated for 100 s, after which it is digitized with 12 bit resolution and recorded. The radiometer is rotated by 45°, and the process is repeated until a 315° rotation has been achieved. The instrument then rotates back to its 0° initial position and
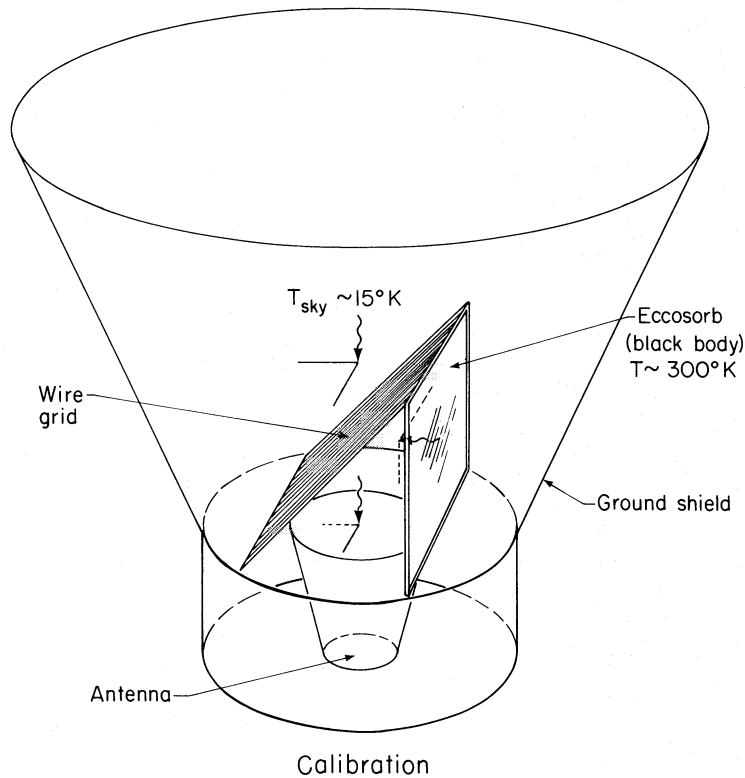

Calibration

Fig. 3.—Sketch of polarized calibrator used.

the cycle repeats. The system is automated and runs unattended except for cleaning and occasional repair.

A typical tape contains about 2 weeks of data before being analyzed. After the analysis these data are added to a library tape containing all previous data. Time is recorded from a crystal controlled clock for later binning of data and correlation of time related events. Data taken during periods of rain or dew are deleted and the humidity is recorded, allowing an additional check of contaminated data.

The northern declination data are taken from the Lawrence Berkeley Laboratory, at a latitude of 38° N. During periods of rain the equipment is either removed or covered. Southern declination data were taken from the Naval Air Base at the Jorge Chavez airport in Lima, Peru, latitude 12° S during 1979 March. These measurements were made along with our U-2 experiment to measure the intensity anisotropy. Although heat, dust, power failures, and logistics made the southern data-taking less than optimal, useful data were obtained.

In both hemispheres the instrument was aligned along the north-south direction so that Q and U were properly defined. The instrument is always tilted along the north-south direction, so that as the Earth sweeps the antenna beam along a constant declination the proper orientation of Q and U is maintained. During a typical run the instrument was pointed toward a fixed declination for 2 weeks with a calibration at the beginning and the end of the run. Multiple runs are taken at most declinations. Figure 4 shows the sky coverage obtained from both the northern and southern hemispheres. In total, 11 declina-

tions were surveyed, ranging from $-37°$ to $+63°$ declination.

e) Wobble Correction

When the instrument is tilted away from the local vertical, the gravitational torque on the radiometer causes stress on the components. This leads to a modulated offset with the same period as the instrumental rotation. A true polarized signal would have a period which is one-half of the rotation period. Rotation by a full 360° cycle in 45° steps would appear to allow complete cancellation of this effect. However, there is a residual second order effect at the 1% level, apparently caused by the mechanical asymmetry of construction, which adds a constant term to both Q and U. The mechanical nature of this wobble was verified by physically rotating the instrument by 180° and noting that the DC (average) level of Q and U reversed sign.

For the northern hemisphere runs, the typical wobble correction is a few tenths of a millikelvin. During the southern hemisphere measurements, the instrument was in a different configuration. In addition, a bolt worked loose during data taking at $\delta = -37°$, causing a false polarized signal of about a millikelvin. The errors for the $\delta = -37°$ data were increased in an effort to allow for the possible systematic errors caused by the larger wobble. It is important to note that this correction is only to the average level and does not affect the time dependence of the data. For the 38° declination data where there is essentially no wobble correction, the DC (average) level is
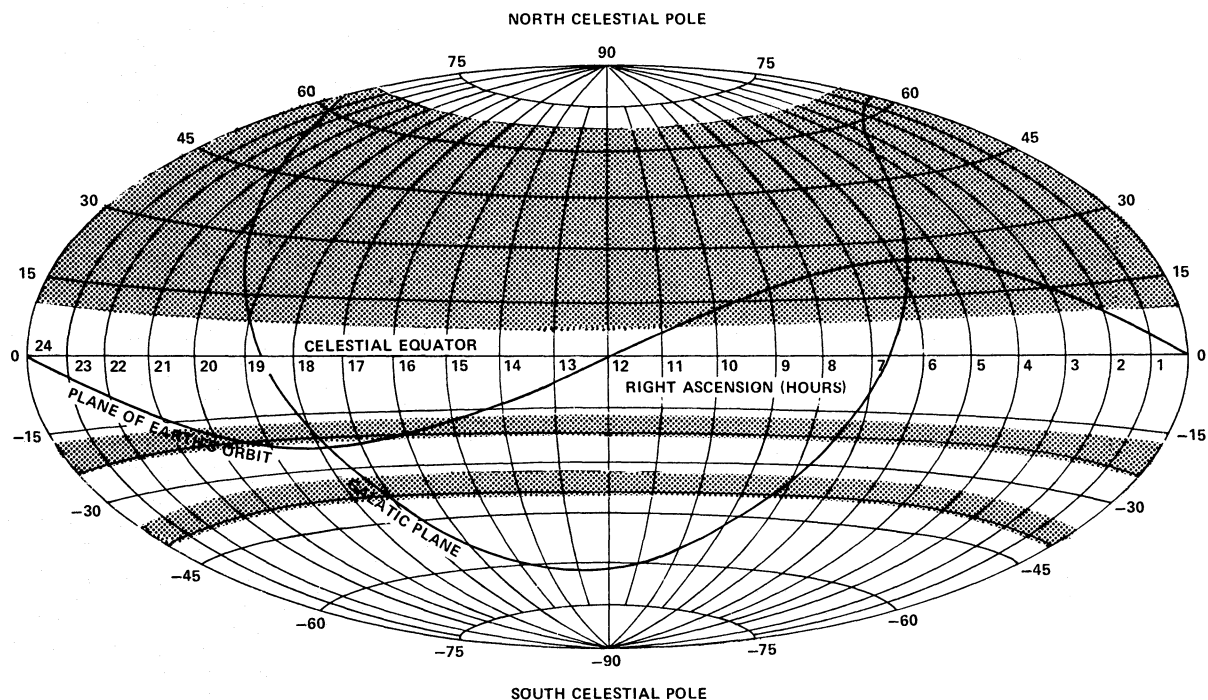

FIG. 4.—Shaded areas show sky coverage achieved in the experiment. Northern declination scans were taken from Berkeley while the southern declination scans were made from Lima, Peru.

consistent with zero, 10 ± 60 μK for Q and 30 ± 60 μK for U.

To make the correction, the northern and southern hemisphere data are analyzed separately. A least-squares fit is made to the wobble versus DC level, assuming a linear relationship and forcing the fit through the origin. The fit is made separately for Q and U in the northern hemisphere runs. A linear relationship is expected because of the mechanical nature of the effect. The data and best fit are shown in Figure 5.

f) Data Reduction

To eliminate the instrumental offset (average DC output) and to obtain both components of linear polarization, the instrument is rotated in 45° increments about the horn axis. A basic rotation cycle produces eight values $S_1, \ldots, S_8$, corresponding to rotation positions 0°, 45°, ..., 315°. The offset is constant with rotation angle (except for the wobble which changes sign under rotation by 180°, while any signal indicative of a true polarization would reverse sign upon rotation of the instrument by 90°. Q and U can thus be calculated as follows:

$$Q = (S_1 - S_3 + S_5 - S_7)/4 , \qquad (9)$$

$$U = (S_2 - S_4 + S_6 - S_8)/4 . \qquad (10)$$

The offset is calculated as the average of $S_1, \ldots, S_8$.

Sidereal time is calculated for each value of Q and U from the recorded universal time. A least-squares fit is made to Fourier components with periods of DC (constant) 24, 12, 8, 6, and 4.8 hours for Q and U at each declination observed. Q and U are binned in hourly
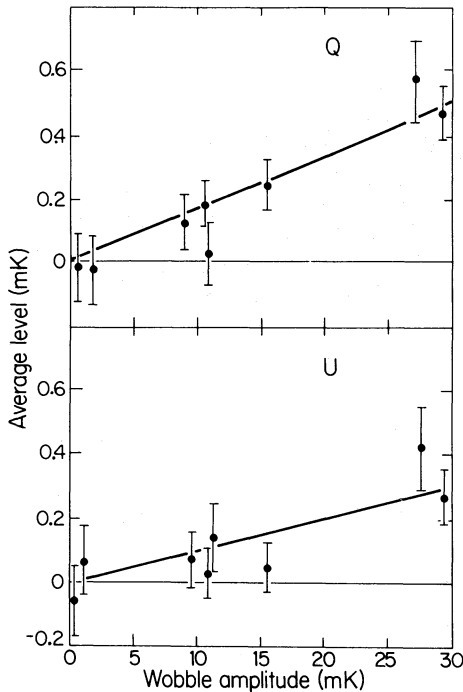

Fig. 5.—Average value of Stokes parameters Q and U versus instrument wobble amplitude for other than vertical looking runs.

sidereal bins, and time plots are made. Global fits are constructed by making a least-squares fit to the hourly bins at each declination, using a series of spherical harmonics as fitting functions.

g) Data Deletion

Deleted or edited data fall into two categories: data which can be eliminated because of known causes (Sun overhead, rain, cleaning ground shield), and data which have obvious nonstatistical behavior of unknown origin. The latter category is somewhat more difficult to quantify in terms of a rejection threshold. Our philosophy is to use all data which are not "obviously" bad, so as not to bias the results.

A diagnostic program is run on the data to test their statistical properties. Table 3 lists the statistical tests performed. In theory, the minimum detectable signal is inversely proportional to the square root of the integration time. This integration test is of particular importance, as it tells us whether or not the data "integrate down" properly. The test is included in the diagnostic program and a sample is shown in Figure 6. The $(N)^{-1/2}$ line is drawn in for comparison.

VI. BACKGROUNDS

There are two approaches in dealing with extraneous backgrounds: either subtract the background emission in the data analysis, or design the experiment to avoid or eliminate the backgrounds. We have adopted the latter philosophy.

a) Galactic and Extragalactic

Diffuse galactic emission is dominated by synchrotron radiation and emission from ionized hydrogen (H II). Synchrotron emission is typically 10–50% linearly polarized, while H II emission is not. Synchrotron emission is thus more relevant as a background. Figure 7 gives an estimate of the total synchrotron emission at 33 GHz based on low frequency surveys (Witebsky 1978). Surveys at low frequency have been made which measure the polarization (Berkhuijsen 1971, 1972; Brouw and Spoelstra 1976). Utilizing the 1411 MHz polarization

TABLE 3

STATISTICAL TESTS OF DATA PERFORMED

| Type of Test	Description
Fourier transform	Test for spurious periodic signals
Run test	Test for random nature of data above and below mean
Gaussian statistics	Check for Gaussian nature of data and look for nonstatistical behavior in tails of distribution
Integration test	Check for low level systematic errors by plotting rms fluctuations of binned data against number of data points in each bin. The fluctuations should average down inversely as the square root of the number of data points in each bin.
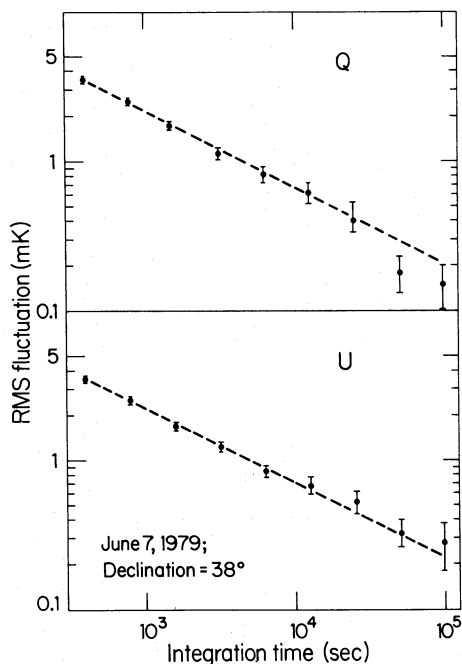
FIG. 6.—RMS fluctuations versus integration time. The $1/t^{1/2}$ line is drawn in for comparison.

survey of Brouw and Spoelstra, the polarized emission at 33 GHz was estimated. Figure 8 shows a contour map estimation of the total polarized signal based on their data. The extrapolation assumes $T_A \sim v^{-2.8}$ with errors likely to be no more than a factor of 2. Because the beam pattern of the antenna is fairly broad, extragalactic sources are negligible at the 0.1 mK level for all known sources.

b) Earth

The earth is a strong source of thermal microwave radiation and, if viewed directly, would have an antenna temperature of 300 K. This radiation is unpolarized, but the slightly asymmetric antenna response with polarization could result in an apparent signal from the Earth. The measured antenna pattern convolved with the theoretical diffraction past the conical ground shield predicts that the apparent signal from the Earth should be less than 0.1 mK for vertical data, and less than 0.2 mK when the apparatus is tilted by 25°, which was the maximum tilt angle used. This apparent signal should be essentially constant, since the temperature and hence emission from the Earth typically varies less than 3% during a 24 hour period.

We performed a test of the sidelobe and diffraction calculation by tilting the apparatus northward 25°
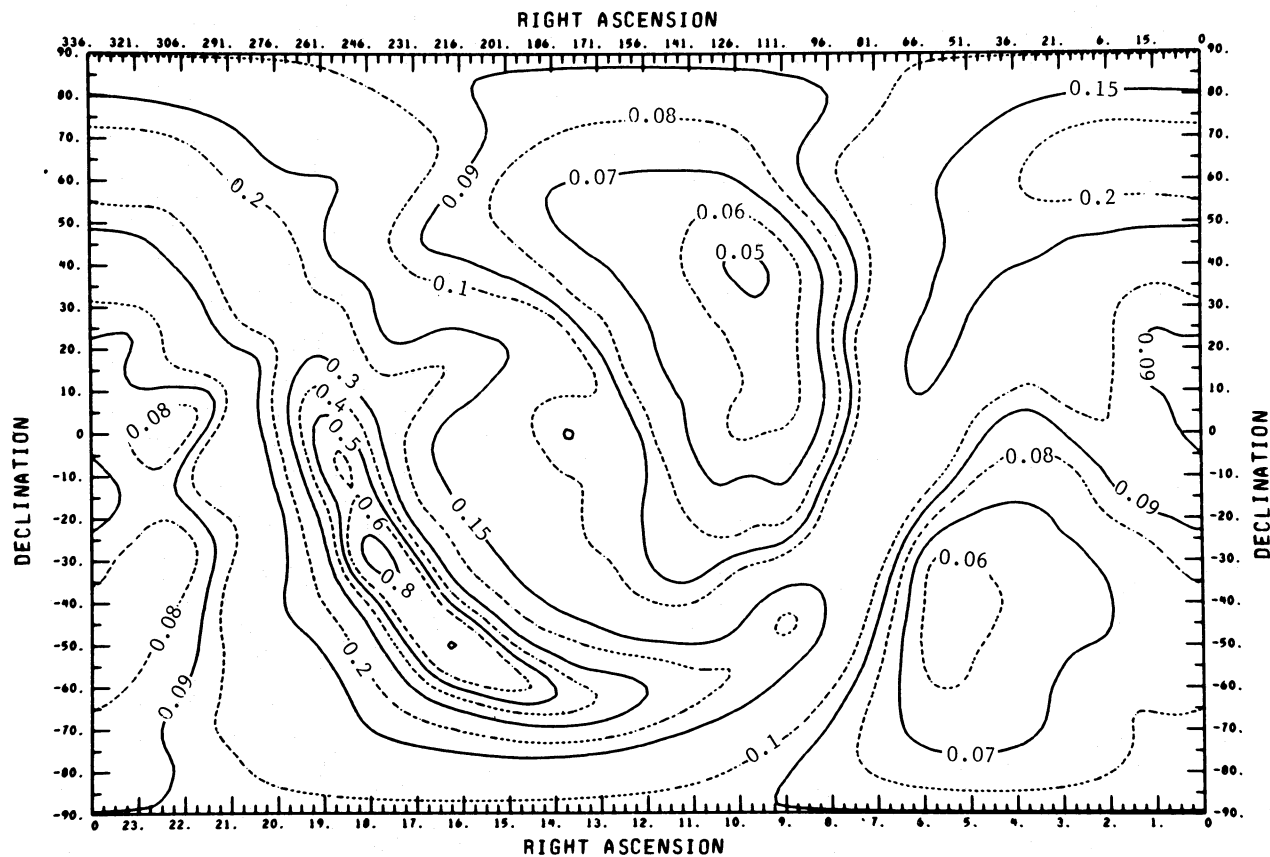

FIG. 7.—Contour map of total estimated galactic synchrotron emission at 33 GHz obtained from lower frequency measurements. Levels are in millikelvins.
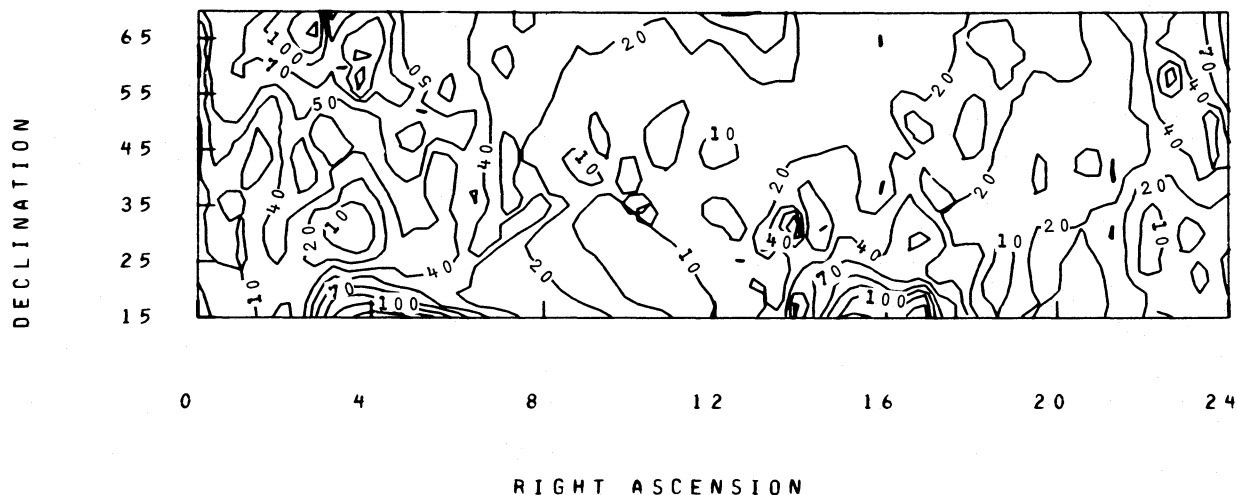
FIG. 8.—Contour map of estimated polarized galactic synchrotron emission at 33 GHz based upon the survey of Brouw and Spoelstra (1976). Levels are in microkelvins.

toward a hill rising about 8° above the horizon and then periodically erecting a large ground shield. The results of this test show that the Earth in the antenna sidelobes contributes no more than 0.24 ± 0.17 mK in this extreme case. We expect that for most of the data the Earth-contributed signal is much lower than the limit set for this large tilt and is therefore negligible.

c) Solar System Sources

The Sun and Moon are a potential background, because small differences in the antenna response pattern to differing polarization states of powerful unpolarized sources can produce small signals in the instrument. For this reason data are ignored when these objects are close to the beam axis. The induced signal is less than 0.1 mK when the Sun is more than 30° from the beam axis, while the corresponding angle for the Moon is 20°.

d) Satellites

A satellite broadcasting at 33 GHz would present a serious background. Fortunately, technology has not progressed to this point, although in several more years this may no longer be the case. A list of broadcasting sources from ECAC (Electromagnetic Compatibility Analysis Center) in Annapolis, Maryland, shows that we are relatively safe from this type of man-made radiation.

e) Dust

Solar system (zodiacal) and galactic dust do not produce significant polarized signals at our observing frequency. Infrared balloon-borne measurements indicate that the total intensity should be well below 0.1 mK everywhere except in certain isolated regions near the galactic plane (Owens, Muehlner, and Weiss 1979). The polarized component would be substantially less.

f) Atmosphere

The atmosphere has an equivalent antenna temperature of about $T_A = 12$ K. Fortunately the emission is not significantly polarized at our frequency. Fog does not appear to be a problem except when it condenses on the rain shield, and data taken during periods of heavy fog or rain are eliminated. Although scattered sunlight is significantly polarized at optical wavelengths, very little is scattered in the microwave region because the scattering cross section is inversely proportional to the fourth power of the wavelength.

g) Terrestrial Magnetic Fields

Because the Faraday rotation switch (FRS) is magnetically controlled, perturbations in the switching field caused by local fields can be a problem. From knowledge of the switch coil geometry and winding, the switching field is approximately $H = 9.2$ gauss. Measurements of the local environment at Berkeley with a Hall probe magnetometer show the local field is essentially that of the Earth with a total magnitude 0.5 ± 0.1 gauss in agreement with USGS map showing $|B| = 0.51$ gauss. Because the ferrite in the FRS has a magnetization dependent absorption, any external magnetic field combined with a misalignment of the ferrite about the physical rotation axis of the equipment could cause a signal. For this reason the FRS was magnetically shielded with several layers of 4 mil mu-metal foil. Measurements show that a single layer of mu-metal reduces transverse fields by a factor of 10^2 and longitudinal fields by a factor of 10. Tests with a Helmholtz pair of coils (separation equals radius) along three axes at fields up to 10 gauss show that the induced signal caused by the Earth is less than 0.08 mK at the 95% confidence level.

h) Depolarization Processes

Consideration must be given to processes which could reduce or depolarize an initially polarized signal.

Since a plasma in a magnetic field becomes birefringent, a plasma in a turbulent magnetic field could be a possible source of depolarization tending to randomly rotate the polarization vector. Table 4 lists the rotation expected from various sources at our frequency. With the exception of an ionized dense universe and a global magnetic field, all known effects are small.

An interesting geometrical depolarizing effect has been suggested by Brans (1975). In this case, an axisymmetric universe causes a scrambling of polarization due to the changing geometry of the universe. This effect has been shown to be small for "reasonable" models of the universe (Caderni *et al.* 1978*b*).

V. MEASURED DATA AND FITTED PARAMETERS

a) Measured Data

Table 5 gives a list of the data and errors at each declination surveyed. These data have been corrected for the temperature dependence of the Faraday rotation switch and for the instrument wobble in runs where the apparatus was not pointed vertically. The northern hemisphere data consist of several runs at each declination which have been merged. Figure 9 shows the data in graphical form at each declination. Because of the restrictions imposed by contamination from the Sun and the limited time in the southern hemisphere, the errors are not equal for each declination. The quoted errors are actual rms errors, based on the scatter of repeated measurements.

b) Spherical Harmonic Fits

A least-squares fit to various spherical harmonics is made using the binned hourly data presented in Table 5. The fitting functions, amplitudes, and errors are shown in Table 6. Independent fits are made to the average, dipole, quadrupole, and octopole spherical harmonics. None of the fitted coefficients is significant, with only the fitted coefficient of $\cos^2 \delta \sin 2\alpha$ for U more than 2 standard deviations from zero.

A fit to the null hypothesis (no polarization) yields a chi-squared of 279 with 264 degrees of freedom (DOF)

and a corresponding confidence level of 25% for Q and a chi-squared of 265 with 264 DOF and a confidence level of 47% for U. In addition, the model of Rees gives a definite prediction as to the functional form of Q and U for a model of anisotropic expansion with a given axis of symmetry (Nanos 1979). Table 7 summarizes the best fit to this model. While the model produces a fairly good fit to the data, it is not significant. *We have found no significant evidence for linear polarization over any of the areas surveyed.*

c) Comparison to Previous Measurements

There have been two previous measurements of the polarization of the cosmic background radiation, Nanos (1979) and Caderni *et al.* (1978*a*), both with null results. Nanos performed a polarization experiment similar to this one in 1973 at a wavelength of 32 mm for one declination of $\delta = 40°$. Caderni *et al.* used a balloon-borne infrared spectrometer operating at a wavelength of 0.5–3 mm, but were forced to terminate after only 4 hours of data taking. Because of the limited sky coverage in both experiments, these data were not fitted to spherical harmonics. The results of Nanos and Caderni *et al.* are summarized in Table 8. Although Nanos's data show a significant (5 σ) average value for Q and U, this was interpreted as sidelobe pickup from a nearby building. The work described here represents about an order of magnitude improvement over previous measurements.

VI. ASTROPHYSICAL INTERPRETATION

a) Limits on Anisotropic Models

The polarization limits obtained in this experiment can be used to set limits on the types of models useful in describing the universe, as well as physical processes which can occur. In general, any model which produces an intrinsic intensity anisotropy in the background radiation will also produce a polarization. Intrinsic anisotropy refers to that which is not produced by our own particular frame of reference and which is present prior to the time of decoupling. Examples of intrinsic anisotropies include rotation of the universe and anisotropic expansion. Examples of anisotropies which are *not* intrinsic include local inhomogeneities (masses), local gravity waves, and the motion of our Galaxy. These latter anisotropies would not be expected to produce any polarization. As stated before, one advantage of this experiment is that it is only sensitive to intrinsic anisotropies; any perturbations present in the intensity which are simply due to our peculiar reference frame do not produce a polarization and thus need not be subtracted away.

The degree of polarization induced by a given intrinsic anisotropy depends on the time at which decoupling occurred, since this sets the time scale on which matter and radiation interact. More specifically, the polarization depends on the ionization fraction as a function of time. Two cases will be considered in this regard. In case I, decoupling occurs at a Z of 1500 with no reionization at later times. In case II, decoupling occurs at a Z of 1500, but matter is later reionized at a Z of 7, possibly

TABLE 4

FARADAY ROTATION AND DEPOLARIZATION[a]
($\Delta\phi \approx 70NBr, \lambda = 0.91$ cm)

Source	N (cm^{-3})	B (gauss)	r (pc)	$\Delta\phi$ (rad)
Galaxy	10^{-3}	10^{-5}	10^4	$< 10^{-2}$
Ionosphere	10^6	1	10^{-11}	$< 10^{-3}$
Extragalactic[b]	10^{-5}	B	10^{10}	$\lesssim 10^7 B$
Extragalactic[c]	10^{-9}	B	10^{10}	$\lesssim 10^3 B$
Solar wind	1	10^{-4}	10^{-3}	$< 10^{-5}$

[a] Plane of polarization rotated by $\Delta\phi \approx 81\lambda^2 \int N(r)B(r) \cos \theta(r) dr$, where λ is the wavelength in cm, N is the electron density per cm^3, B is in gauss, θ is the angle between $\bar{B}$ and the direction of propagation, and r is in parsecs (1 pc $\sim 3.1 \times 10^{18}$ cm ~ 3.3 lt-yr).
[b] Assuming complete ionization in a critically dense universe with a universal magnetic field B.
[c] As in (*b*) except ionized fraction = 10^{-4}.

TABLE 5

DATA AND ERRORS AT EACH DECLINATION

DECLINATION	R.A.	Q	SIGMA Q	U	SIGMA U
-37.00	.50	.69	.61	.72	.53
-37.00	1.50	1.22	.53	.19	.58
-37.00	2.50	-.08	.74	.88	.86
-37.00	3.50	-.23	.71	-.06	.79
-37.00	4.50	.38	.80	.25	.75
-37.00	5.50	-.32	.60	1.67	.87
-37.00	6.50	-.12	.68	.47	.70
-37.00	7.50	-.29	.83	.70	.93
-37.00	8.50	-.33	.62	-.20	.74
-37.00	9.50	-.17	.74	-.48	.85
-37.00	10.50	-1.27	.91	.97	.96
-37.00	11.50	.61	.94	-.11	.71
-37.00	12.50	-1.11	1.02	-.20	.90
-37.00	13.50	-.14	.81	-.28	.68
-37.00	14.50	-1.81	1.05	.18	.89
-37.00	15.50	-1.69	.87	-.23	.96
-37.00	16.50	-.03	.87	.86	1.08
-37.00	17.50	1.29	.80	-.13	1.14
-37.00	18.50	-1.00	.81	-.90	.66
-37.00	19.50	1.00	.80	-1.21	.79
-37.00	20.50	.13	.63	.12	.64
-37.00	21.50	.13	.57	-1.45	.63
-37.00	22.50	.63	.56	-.47	.52
-37.00	23.50	.47	.49	-.47	.49
-20.00	.50	-1.16	1.52	-.23	1.20
-20.00	1.50	.64	.71	.55	.99
-20.00	2.50	1.14	1.23	-.08	1.33
-20.00	3.50	-1.03	1.22	-2.61	1.36
-20.00	4.50	-1.34	1.03	-2.52	1.56
-20.00	5.50	1.35	1.68	1.37	1.22
-20.00	6.50	1.01	1.75	.67	1.89
-20.00	7.50	1.56	1.40	-.23	1.12
-20.00	8.50	.14	1.51	1.95	1.04
-20.00	9.50	.84	.93	-2.09	1.20
-20.00	10.50	-1.82	1.21	-.58	.96
-20.00	11.50	-.27	2.06	-.28	1.11
-20.00	12.50	3.07	1.37	-.43	1.00
-20.00	13.50	-1.61	1.89	-1.53	1.63
-20.00	14.50	.94	1.60	-1.09	1.22
-20.00	15.50	.54	1.83	-1.66	2.71
-20.00	16.50	1.92	2.34	-3.11	2.94
-20.00	17.50	-.87	2.00	1.53	1.99
-20.00	18.50	-.86	1.36	.35	1.58
-20.00	19.50	-1.07	.87	2.05	.97
-20.00	20.50	-1.13	1.32	-.61	.87
-20.00	21.50	-1.41	.99	-.43	.85
-20.00	22.50	.31	1.96	1.62	1.83
-20.00	23.50	.31	1.48	1.62	1.30
13.00	.50	.72	.52	.81	.52
13.00	1.50	-.88	.56	-.28	.56
13.00	2.50	.07	.57	-.43	.57
13.00	3.50	-.13	.57	.71	.57
13.00	4.50	-.69	.59	1.15	.57
13.00	5.50	1.14	.65	-.10	.65
13.00	6.50	-.30	.50	.72	.64
13.00	7.50	.71	.56	-.60	.57
13.00	8.50	.35	.49	.17	.60
13.00	9.50	.08	.59	-.31	.49
13.00	10.50	-.21	.66	.13	.55
13.00	11.50	.35	.65	-.28	.51
13.00	12.50	.17	.71	-1.10	.72
13.00	13.50	-.06	.69	.08	.73
13.00	14.50	-.65	.64	-1.61	.61
13.00	15.50	-.99	.64	-.19	.77
13.00	16.50	.36	.67	.06	.83
13.00	17.50	-1.12	.61	-.19	.69
13.00	18.50	.93	.61	-.25	.64
13.00	19.50	-.46	.65	-1.01	.74
13.00	20.50	.98	.57	.37	.57
13.00	21.50	-1.17	.57	.17	.68
13.00	22.50	1.17	.63	-.75	.58
13.00	23.50	-.74	.54	.53	.57
18.00	.50	-.39	.46	-.03	.50
18.00	1.50	-.67	.57	-.70	.46
18.00	2.50	.49	.56	-.43	.55
18.00	3.50	-.64	.44	-.13	.48
18.00	4.50	.02	.55	-.32	.50
18.00	5.50	-.35	.51	-.05	.49
18.00	6.50	-.07	.63	.85	.55
18.00	7.50	-.36	.59	-.19	.65
18.00	8.50	-.02	.44	-.26	.54
18.00	9.50	-.22	.57	.51	.48
18.00	10.50	-.31	.55	-.27	.48
18.00	11.50	-.37	.51	-.63	.50
18.00	12.50	-1.00	.52	.55	.62
18.00	13.50	-1.05	.49	-.78	.53
18.00	14.50	-.48	.45	-.12	.41
18.00	15.50	-.60	.50	1.74	.50
18.00	16.50	-.02	.46	-.54	.48
18.00	17.50	-.29	.53	-.63	.49
18.00	18.50	-.53	.49	-.09	.46
18.00	19.50	-.11	.55	-.18	.42
18.00	20.50	-.60	.61	-.52	.61
18.00	21.50	-.30	.48	-.49	.48
18.00	22.50	-.07	.49	-.14	.52
18.00	23.50	-.28	.47	-.47	.54

TABLE 5—Continued

DECLINATION	R.A.	Q	SIGMA Q	U	SIGMA U
23.00	.50	.28	.50	.65	.57
23.00	1.50	-.64	.47	.31	.53
23.00	2.50	-.01	.46	.15	.46
23.00	3.50	-.35	.49	-.15	.43
23.00	4.50	.01	.49	.25	.45
23.00	5.50	.84	.42	-.38	.50
23.00	6.50	.48	.54	.76	.48
23.00	7.50	.33	.52	.39	.55
23.00	8.50	-.26	.60	.24	.35
23.00	9.50	.80	.59	-.37	.61
23.00	10.50	.15	.50	-.29	.52
23.00	11.50	.30	.39	-.32	.53
23.00	12.50	-.47	.50	.10	.42
23.00	13.50	-.66	.48	-.26	.42
23.00	14.50	-.34	.43	.14	.47
23.00	15.50	-.40	.50	-.46	.59
23.00	16.50	-.70	.49	.06	.50
23.00	17.50	-.35	.43	-.02	.50
23.00	18.50	-.38	.38	.12	.42
23.00	19.50	-1.55	.55	-.41	.50
23.00	20.50	.37	.58	-.07	.48
23.00	21.50	-.05	.43	.53	.51
23.00	22.50	.59	.45	-1.01	.39
23.00	23.50	.19		.63	
28.00	.50	.74	.56	.53	.53
28.00	1.50	.73	.40	.22	.50
28.00	2.50	-.58	.48	-.15	.45
28.00	3.50	-.40	.54	-.33	.40
28.00	4.50	-.30	.59	.69	.52
28.00	5.50	-.12	.45	.46	.42
28.00	6.50	-.10	.45	.39	.49
28.00	7.50	-.26	.42	-.32	.48
28.00	8.50	-1.11	.38	.70	.47
28.00	9.50	.05	.52	.25	.45
28.00	10.50	.01	.56	-.02	.50
28.00	11.50	1.08	.54	-.12	.52
28.00	12.50	-1.00	.43	.52	.50
28.00	13.50	-.22	.48	.61	.45
28.00	14.50	-.08	.39	-.33	.52
28.00	15.50	-.50	.48	-.05	.49
28.00	16.50	.15	.48	.15	.53
28.00	17.50	-.08	.40	.37	.55
28.00	18.50	.75	.38	-.22	.46
28.00	19.50	-.00	.46	.01	.47
28.00	20.50	.57	.55	-.28	.46
28.00	21.50	-.30	.45	.49	.57
28.00	22.50	-.13	.51	-1.76	.53
28.00	23.50	.37		.07	

DECLINATION	R.A.	Q	SIGMA Q	U	SIGMA U
38.00	.50	.27	.30	.03	.32
38.00	1.50	-.19	.29	.45	.35
38.00	2.50	-.10	.31	.17	.30
38.00	3.50	-.53	.30	-.25	.33
38.00	4.50	.25	.37	.42	.32
38.00	5.50	-.10	.37	.37	.32
38.00	6.50	-.11	.37	-.01	.32
38.00	7.50	.07	.32	.21	.36
38.00	8.50	-.19	.30	.03	.32
38.00	9.50	-.20	.32	.39	.33
38.00	10.50	.25	.30	-.16	.32
38.00	11.50	.49	.30	-.11	.30
38.00	12.50	-.02	.30	-.37	.33
38.00	13.50	.03	.30	.05	.27
38.00	14.50	.04	.30	.19	.29
38.00	15.50	-.12	.33	-.09	.32
38.00	16.50	-.22	.31	-.30	.27
38.00	17.50	.54	.31	.67	.30
38.00	18.50	.03	.29	-.09	.31
38.00	19.50	-.18	.31	.14	.26
38.00	20.50	-.17	.30	-.43	.27
38.00	21.50	.17	.31	.41	.28
38.00	22.50	.34	.33	-.60	.27
38.00	23.50	-.08	.32	-.20	
48.00	.50	-.15	.42	-.42	.41
48.00	1.50	-.51	.49	.21	.51
48.00	2.50	-1.00	.42	-.39	.49
48.00	3.50	-.63	.52	-.49	.48
48.00	4.50	.57	.47	-.13	.44
48.00	5.50	-.09	.44	-.44	.43
48.00	6.50	-.10	.50	-.20	.44
48.00	7.50	-.02	.46	.58	.49
48.00	8.50	.24	.39	.08	.48
48.00	9.50	.44	.47	-.23	.43
48.00	10.50	-.07	.42	-.38	.53
48.00	11.50	.57	.49	-.03	.42
48.00	12.50	-1.22	.60	-.26	.49
48.00	13.50	-.29	.40	-.41	.46
48.00	14.50	-.47	.33	-.25	.45
48.00	15.50	-.18	.43	.35	.42
48.00	16.50	1.06	.47	.15	.52
48.00	17.50	-.08	.39	.84	.47
48.00	18.50	1.37	.42	-.20	.43
48.00	19.50	-.13	.38	.56	.48
48.00	20.50	.75	.48	-.14	.47
48.00	21.50	-.30	.42	.75	.49
48.00	22.50	-.27	.39	-.37	.48
48.00	23.50			-.13	

TABLE 5—Continued

DECLINATION	R.A.	Q	SIGMA Q	U	SIGMA U
53.00	.50	.77	.32	.37	.30
53.00	1.50	-.04	.31	.22	.30
53.00	2.50	-.56	.29	-.13	.31
53.00	3.50	.16	.34	.66	.33
53.00	4.50	-.39	.32	-.05	.32
53.00	5.50	-.26	.36	.09	.28
53.00	6.50	.17	.30	-.14	.35
53.00	7.50	-.17	.30	-.26	.30
53.00	8.50	-.44	.31	-.26	.31
53.00	9.50	-.48	.28	-.39	.30
53.00	10.50	-.32	.25	.10	.26
53.00	11.50	-.22	.31	-.04	.35
53.00	12.50	-.18	.30	-.16	.34
53.00	13.50	-.04	.32	-.06	.30
53.00	14.50	-.31	.29	-.46	.28
53.00	15.50	-.17	.30	.78	.30
53.00	16.50	-.32	.32	-.08	.28
53.00	17.50	-.24	.32	-.18	.33
53.00	18.50	-.20	.32	-.41	.30
53.00	19.50	-.49	.29	-.49	.30
53.00	20.50	.56	.30	-.07	.34
53.00	21.50	-.32	.30	-.10	.32
53.00	22.50	-.27	.32	-.34	.32
53.00	23.50	-.22	.31	.15	.32
58.00	.50	.27	.46	.18	.44
58.00	1.50	-.61	.41	-.47	.43
58.00	2.50	.54	.48	-.67	.50
58.00	3.50	-.40	.44	-.30	.45
58.00	4.50	-.30	.40	-.22	.40
58.00	5.50	-.22	.38	-.88	.39
58.00	6.50	.29	.43	.16	.40
58.00	7.50	.65	.42	-.45	.41
58.00	8.50	.02	.42	.05	.40
58.00	9.50	.05	.41	-.04	.40
58.00	10.50	.43	.37	-.68	.38
58.00	11.50	.16	.43	.37	.47
58.00	12.50	-.19	.40	-.11	.39
58.00	13.50	.52	.33	-.37	.37
58.00	14.50	-.05	.37	-.26	.37
58.00	15.50	-.30	.36	-.08	.37
58.00	16.50	-.36	.43	-.18	.35
58.00	17.50	.45	.39	-.17	.39
58.00	18.50	.25	.37	-.65	.37
58.00	19.50	-.66	.41	-.66	.45
58.00	20.50	-.20	.38	-.10	.41
58.00	21.50	-.30	.38	-.44	.37
58.00	22.50	-.28	.41	.33	.41
58.00	23.50	-.51	.44	.32	.36
63.00	.50	-.60	.39	-.08	.36
63.00	1.50	.10	.41	.35	.38
63.00	2.50	-.01	.37	.21	.38
63.00	3.50	-.03	.34	-.14	.35
63.00	4.50	-.07	.38	-.23	.33
63.00	5.50	-.12	.40	.40	.33
63.00	6.50	-.14	.32	-.04	.37
63.00	7.50	.16	.28	-.01	.34
63.00	8.50	.63	.32	-.13	.38
63.00	9.50	-.40	.36	-.23	.34
63.00	10.50	.16	.34	-.07	.36
63.00	11.50	-.36	.32	.15	.35
63.00	12.50	-.05	.33	-.07	.39
63.00	13.50	-.17	.32	.57	.34
63.00	14.50	-.00	.36	.33	.36
63.00	15.50	-.05	.37	-.10	.32
63.00	16.50	-.19	.39	1.34	.34
63.00	17.50	-.39	.38	-.39	.36
63.00	18.50	-.06	.34	-.17	.38
63.00	19.50	-.43	.39	-.05	.36
63.00	20.50	-.06	.39	-.10	.36
63.00	21.50	-.30	.35	-.14	.37
63.00	22.50	-.04	.39	-.52	.41
63.00	23.50	.76	.42	-.19	.43

12
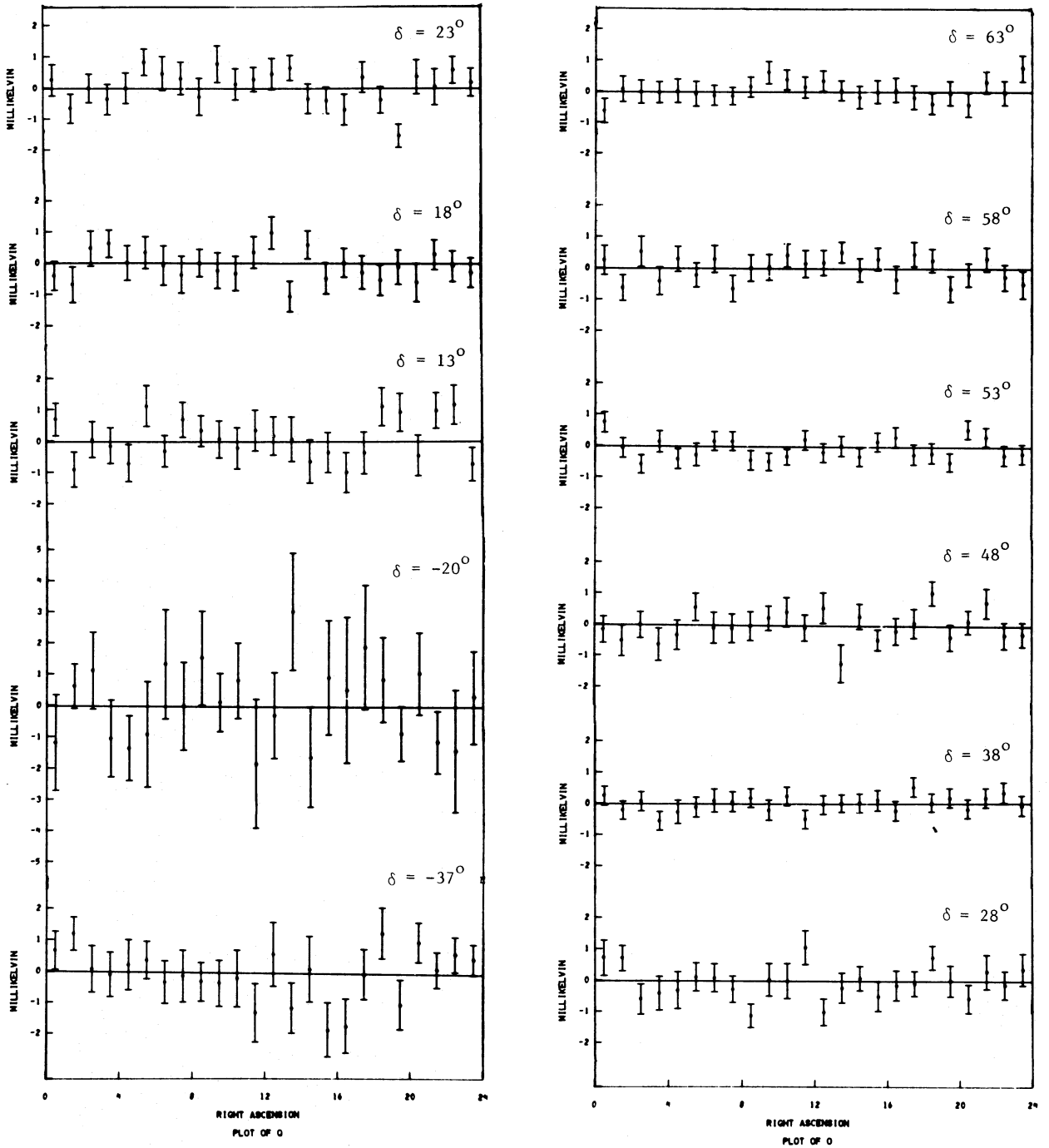
Fig. 9.—Data for each declination surveyed plotted in hourly bins by sidereal time.

13
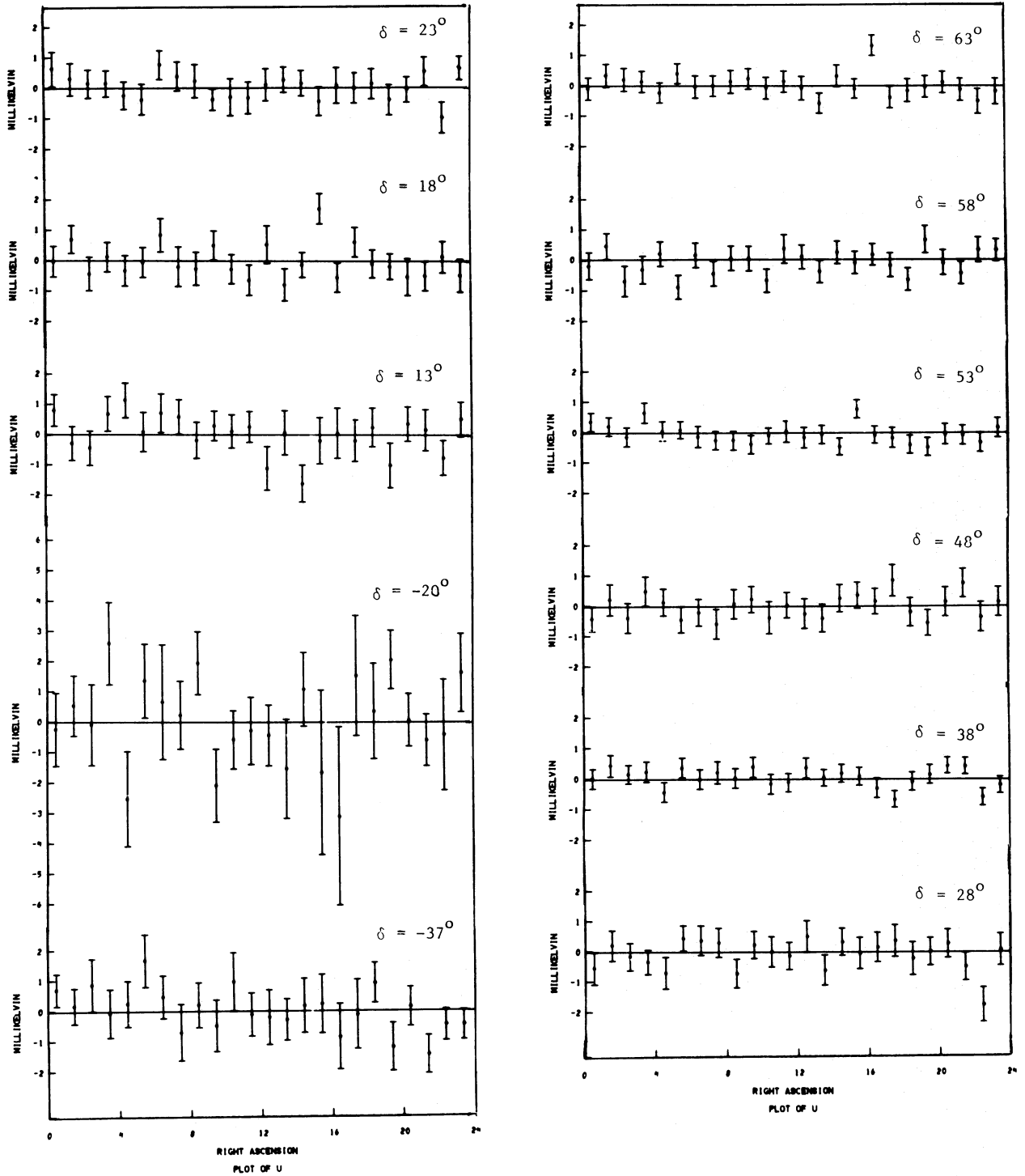
FIG. 9.—*Continued*

TABLE 6

SPHERICAL HARMONIC FITS — INDEPENDENT FITS BY ORDER
(millikelvin)

Fitting Function $P_l{}^m$	Q Fit	U Fit	Error
1	0.00	−0.01	0.03
$\sin \delta$	−0.02	−0.03	0.04
$\cos \delta \cos \alpha$	0.02	0.02	0.05
$\cos \delta \sin \alpha$	0.00	0.08	0.05
$\frac{1}{2}(3 \sin^2 \delta - 1)$	−0.02	−0.05	0.06
$\cos 2\delta \cos \alpha$	−0.05	0.01	0.04
$\cos 2\delta \sin \alpha$	−0.03	0.02	0.04
$\cos^2 \delta \cos 2\alpha$	0.08	−0.06	0.06
$\cos^2 \delta \sin 2\alpha$	−0.10	0.15	0.06
$\frac{1}{2}(5 \sin^3 \delta - 3 \sin \delta)$	0.04	−0.03	0.08
$\frac{1}{4} \cos \delta (5 \sin^2 \delta - 1) \cos \alpha$	−0.02	0.01	0.05
$\frac{1}{4} \cos \delta (5 \sin^2 \delta - 1) \sin \alpha$	−0.06	0.01	0.05
$\cos 2\delta \sin \delta \cos 2\alpha$	0.03	0.01	0.05
$\cos 2\delta \sin \delta \sin 2\alpha$	−0.05	0.08	0.05
$\cos^3 \delta \cos 3\alpha$	−0.01	0.06	0.07
$\cos^3 \delta \sin 3\alpha$	−0.07	0.04	0.08

Fit	$Q: \chi^2$ per DOF	$U: \chi^2$ per DOF
1	279/263 CL = 24%	279/263 CL = 24%
Dipole	279/261 CL = 21%	281/261 CL = 19%
Quadrupole	274/259 CL = 25%	296/259 CL = 6%

corresponding to the era of early galaxy formation. In both cases, the calculations of Peebles (1968) are used for the ionization fraction through the era of decoupling (Negroponte and Silk, 1980; Basko and Polnarev 1980) and critical density is assumed. Table 9 gives the limits that the polarization measurement places on two processes in terms of the cases mentioned.

The calculations of Negroponte and Silk (1980) are used for the limits on anisotropic expansion and large-scale density fluctuations.

b) Comparison to Intensity Measurements

The best limits on the intensity anisotropy other than the first order (motion) anisotropy come from the Prin-ceton and Berkeley anisotropy experiments. The measured value of the first order term and limits on the higher order terms are shown in Table 10.

A direct comparison between polarization and intensity is not possible without a model to connect these two intrinsically different processes. A comparison between polarization and intensity measurements is given in Table 11 for the case of an axisymmetric, anisotropic universe, based on the model of Rees (1968) and the calculations of Negroponte and Silk (1980).

c) Quadrupole Measurement

Fabbri et al. (1980) have recently reported the existence of a possible quadrupole component in the cosmic

TABLE 7

FIT TO ANISOTROPIC AXISYMMETRIC MODEL (Rees)

PREDICTION OF MODEL

$Q = (T_w - T_a)_{max} [\cos^2 \delta (1 - 3/2 \sin^2 \theta_0) + \sin 2\theta_0 \cos \delta \sin \delta \sin (t - \alpha_0 - \pi/2) + \sin^2 \theta_0 (1 - 1/2 \cos^2 \delta) \sin 2 (t - \alpha_0 + \pi/4)];$

$U = -(T_w - T_a)_{max} [\sin 2\theta_0 \cos \delta \sin (t - \alpha_0 + \pi) + \sin^2 \theta_0 \sin \delta \sin 2 (t - \alpha_0)],$

where θ_0 = angle from celestial pole to symmetry axis of universe;
α_0 = right ascension of symmetry axis of universe.

LEAST SQUARES FIT TO MODEL GIVES:

$(T_w - T_a)_{max} = -0.07 \pm 0.04$ mK

$\theta_0 = 40° \pm 20°$

$\alpha_0 = 13 \pm 1.5$ hr

χ^2 per DOF $= \frac{542}{525}$

CL = 30%

TABLE 8

RESULTS OF PREVIOUS MEASUREMENTS

Nanos (1979)
($\delta = 40°$, 15° beamwidth, $\lambda = 32$ mm)

Period	Q Fit (mK)	U Fit (mK)	Error (mK)
Average	−0.67	−0.88	0.14
24 hr	0.52	0.58	0.20
12 hr	0.20	0.45	0.20

Fit to anisotropic model of Rees (1968) yields 1.6 mK 90% C.L. limit

Caderni et al. (1978)
$\delta = -10°$ to $-45°$, $\alpha = 17^h5$ to 20^h5

Q, U < 2 mK, 70% confidence level over area covered.
Data base too small to fit to functional forms

TABLE 9

MODEL CONSTRAINTS FROM POLARIZATION DATA

Model	Case 1 (no reionization)	Case 2 (reionization $z = 7$)
Anisotropic expansion	$\delta h_0/h_0 < 6 \times 10^{-8}$	$\delta h_0/h_0 < 2 \times 10^{-8}$
Density fluctuations (large scale)	$\delta\rho_0/\rho_0 < 1$	$\delta\rho_0/\rho_0 < 2 \times 10^{-3}$

TABLE 10

COMPARISON WITH INTENSITY MEASUREMENTS, DIPOLE AND QUADRUPOLE FIT (mK)

FITTING FUNCTION	INTENSITY[a]		POLARIZATION		
	Fit	Error	Q Fit	U Fit	Error
$\sin\delta$	−0.18	0.39	−0.02	−0.03	0.04
$\cos\delta\cos\alpha$	−2.78	0.28	0.02	0.02	0.05
$\cos\delta\sin\alpha$	0.66	0.29	0.00	0.08	0.05
$\frac{1}{2}(3\sin^2\delta - 1)$	0.38	0.26	−0.02	−0.05	0.06
$\sin 2\delta\cos\alpha$	−0.34	0.29	−0.05	0.01	0.04
$\sin 2\delta\sin\alpha$	0.02	0.24	−0.03	0.02	0.04
$\cos^2\delta\cos 2\alpha$	−0.11	0.16	0.08	−0.06	0.06
$\cos^2\delta\sin 2\alpha$	0.06	0.20	−0.10	0.15	0.06

[a] Smoot and Lubin 1979.

background radiation with an amplitude of $0.9^{+0.4}_{-0.2}$ mK. Their measurements are taken near the peak (0.5–3 mm), and are not directly comparable to our polarization data or past isotropy data for two reasons. First, if the

TABLE 11

COMPARISON OF POLARIZATION AND INTENSITY

Case	P/ϵ[a]
No reheat of plasma	0.04
Reheat at $z = 7$:	
$\Omega_{II} = 1$	0.3
$\Omega_{II} = 0.1$	0.07
Reheat at $z = 40$, $\Omega_{II} = 1$	2
Reheat at $z = 100$, $\Omega_{II} = 1$	0.5

[a] P/ϵ = ratio of polarization to intensity.

spectrum is distorted near the peak as reported by Woody and Richards (1979), then both the dipole and quadrupole amplitude will differ from the lower frequency values (Lubin 1980b). Second, because the data of Fabbri et al. have limited sky coverage, the precise functional form of the anisotropy is not well established. However, if we assume the spectrum is Planckian (blackbody), then the calculations of Negroponte and Silk (1980) indicate that to measure a polarization resulting from the reported anisotropy at our level of sensitivity, the intergalactic medium would need to be near critical density and that there would need to be a significant reionization by a redshift $Z > 7$ for us to see a positive effect at our 0.3 mK 95% confidence level upper limit. Boughn, Cheng, and Williams (1981) have also recently reported a quadrupole component of amplitude 0.54 ± 0.14 mK in $\cos^2\delta\sin 2\alpha$. Unfortunately, this does

not fit the simple axisymmetric anisotropic model of Rees, so the level at which polarization would be expected from such a quadrupole is unknown.

REFERENCES

Basko, M. M., and Polnarev, A. G. 1980, *M.N.R.A.S.*, **191**, 207.
Berkhuijsen, E. M. 1971, *Astr. Ap.*, **14**, 359.
———. 1972, *Astr. Ap. Suppl.*, **5**, 263.
Boughn, S. P., Cheng, E. S., and Wilkinson, D. T. 1981, *Ap. J. (Letters)*, in press.
Brans, C. H. 1975, *Ap. J.*, **197**, 1.
Brouw, W. N., and Spoelstra, T. A. Th. 1976, *Astr. Ap. Suppl.*, **26**, 129.
Caderni, N., Fabbri, R., Melchiorri, B., Melchiorri, F., and Natale, V. 1978a, *Phys. Rev.*, **D17**, 8, 1908.
———. 1978b, *Phys. Rev.*, **D17**, 8, 1901.
Cheng, E. S., Saulson, P. R., Wilkinson, D. T., and Corey, B. E. 1979, *Ap. J. (Letters)*, **232**, L139.
Chu, T. S., Gans, M. J., and Legg, W. E. 1975, *Bell. Sys. Tech. J.* **54**, 10, 1665.
Collins, C. B., and Hawking, S. W. 1973, *M.N.R.A.S.*, **162**, 307.
Corey, B. E., and Wilkinson, D. T. 1976, *Bull. A.A.S.*, **8**, 351.
Fabbri, R., Guidi, I., Melchiorri, F., and Natale, V. 1980, *Phys. Rev. Letters*, **44**, 23.
Gorenstein, M. V., and Smoot, G. F. 1981, *Ap. J.*, **245**, in press.
Hawking, S. 1969, *M.N.R.A.S.*, **142**, 129.
Kraus, J. D. 1966, *Radio Astronomy* (New York: McGraw-Hill).
Lubin, P. M. 1980a, Ph.D. thesis, U. C. Berkeley.
———. 1980b, Internal group memo, unpublished, NASA note number 411.
Lubin, P. M., and Smoot, G. F. 1979, *Phys. Rev. Letters*, **42**, 2, 129.
Mach, E. 1893, *The Science of Mechanics* (2d ed.; Open Court Publishing Co.).
Nanos, G. P. 1974, Ph.D. thesis, Princeton University.
———. 1979, *Ap. J.*, **232**, 341.
Negroponte, J., and Silk, J. 1980, *Phys. Rev. Letters*, **44**, 1433.
Owens, D. K., Muehlner, D. J., and Weiss, R. 1979, *Ap. J.*, **231**, 702.
Peebles, P. J. E. 1968, *Ap. J.*, **153**, 11.
Penzias, A. A., and Wilson, R. W. 1965, *Ap. J.*, **142**, 419.
Rees, M. J. 1968, *Ap. J. (Letters)*, **153**, L1.
Shurcliff, W. A., and Ballard, S. S. 1962, *Polarized Light* (New York: Van Nostrand).
Smoot, G. F., Gorenstein, M. V., and Muller, R. A. 1977, *Phys. Rev. Letters*, **39**, 14, 898.
Smoot, G. F., and Lubin, P. M. 1979, *Ap. J. (Letters)*, **234**, L117.
Weinberg, S. 1972, *Gravitation and Cosmology: Principles and Applications of the General Theory of Relativity* (New York: Wiley).
Witebsky, C. 1978, Internal group memo, unpublished, NASA note number 361.
Woody, D. P., and Richards, P. L. 1979, *Phys. Rev. Letters*, **42**, 14, 925.

PHILIP M. LUBIN and GEORGE F. SMOOT: Building 50-Room 230, Lawrence Berkeley Laboratory, Berkeley, CA 94720